Article

Fire occurrences and greenhouse gas emissions from deforestation in the Brazilian Amazon

Claudia Arantes Silva [1, *], Giancarlo Santilli [2], Edson Eyji Sano [3] and Giovanni Laneve [4]

[1] Universidade de Brasília (UnB), Instituto de Geociências (IG); silvaclaudia.geol@gmail.com
[2] Universidade de Brasília (UnB), Faculdade Gama (FGA); santilli@aerospace.unb.br
[3] Embrapa Cerrados; edson.sano@embrapa.br
[4] Sapienza University of Rome, Scuola di Ingegneria Aerospaziale; giovanni.laneve@uniroma1.it
[*] Correspondence: silvaclaudia.geo@gmail.com

Abstract: This work presents the dynamics of forest clearing in the Brazilian Amazon during the period 2006–2019 in which includes the approval of the new Brazilian Forest Code in 2012. The study was carried out in the Brazilian Amazon, Pará State and in the municipality of Novo Progresso (Pará State). The analysis was based on deforestation and fire hotspot datasets issued by the Brazilian Institute for Space Research (INPE), produced based on optical and thermal sensors onboard different satellites. Deforestation data was also used to assess greenhouse gas (GHG) emissions from the slash-and-burn practices. The work showed a good correlation between the occurrence of fires in the newly deforested area in the municipality of Novo Progresso and the slash-and-burn practices. The same trend was also observed in the Pará State, suggesting a common practice along the deforestation arch. The study indicated positive coefficients of determination of 0.72 and 0.66 between deforestation and fire occurrences for the municipality of Novo Progresso and Pará State, respectively. The increased number of fire occurrences in the primary forest suggests possible ecosystem degradation. Deforestation reported for 2019 surpassed 10,000 km^2, a significant intensification comparatively higher than the previous ten years which was on an average of 6,760 km^2. The steady increase of deforestation in the Amazon after 2012 has been a worldwide concern because of the forest loss itself as well as the massive GHG emitted in the Brazilian Amazon (295 million tons of net CO_2 equivalent in the year 2019). Better correlation of deforestation and fires occurrences reported from satellite images confirmed the slash-and-burn practice and the secondary effect of deforestation, which degrades primary forest surrounding the deforested areas.

Keywords: Amazon rainforest; forestry degradation; greenhouse gas emission; remote sensing application.

1. Introduction

Global efforts have been enforced to preserve Earth's ecosystems and to mitigate climate changes, including reductions of deforestation and forest degradation [1,2]. Brazilian Amazon is one of the most endangered ecosystems. A deep understanding of this ecosystem, including its carbon cycle, is essential to know the adaptability of environment to microclimate changes [3]. The Brazilian Amazon, with about 5.2 million square kilometres, covers the states of Acre (AC), Amapá (AP), Amazonas (AM), Maranhão (MA), Mato Grosso (MT), Pará (PA), Rondônia (RO), Roraima (RR), and Tocantins (TO) and occupies about 60% of the Brazilian territory (Figure 1A). Human occupation in this region has claimed large areas of the original forest for settlement, beef production, crop plantation, and hydropower generation [4–12], especially in a region known as deforestation arch. This arch-shaped region is located in the southernmost part of the Brazilian Amazon rainforest and shows the highest occurrence of forest clearings [13] and occupation [14,15]. It covers about 1.71 million square kilometres which is 33% of original Brazilian Amazon. The region stretches from the southeast of Pará State to the north of Acre State, concentrating 77% of total deforestation of the Brazilian rainforest, mostly for soybean crops and cattle ranching [5,15,16]. Figure 1B shows the

annual deforestation over the Pará State and the Brazilian Amazon, as estimated by the National Institute for Space Research (INPE), from 1988 to 2019. This institution defines deforestation as the clear-cut conversion of the primary forest by human activities, detected by the Earth Observation satellite optical sensors [13].
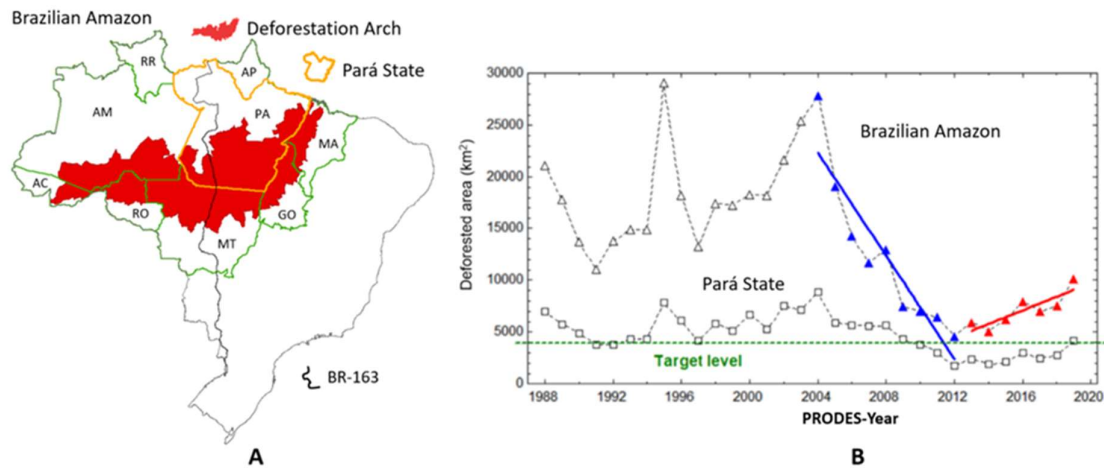
Figure 1. (A) Brazilian states with rainforest and the deforestation arch (red area). (B) Total deforestation area in the Brazilian Amazon (triangle) and in the Pará State (square), according to the INPE's PRODES project.

Since 2006, the highest levels of deforestation in the Brazilian Amazon are found in the Pará State, reaching about 5,000 km^2 in 2019. It can also be seen in Figure 1B that the deforestation trend in the Pará is similar to that of the entire Brazilian Amazon. In this state, forest disturbances are located mainly in the south, southwest, and east borders, covering approximately 550,000 km^2. The largest annual deforestation in the Brazilian Amazon occurred in 1995, surpassing 29,000 km^2. A second peak occurred in the period 2002–2004, with an average of 24,939 km^2. From 2004 to 2012, there was a sharp decrease in annual deforestation rates, as indicated by the blue line in Figure 1B (correlation higher than 80%). Voluntary REDD+ (Reduce Emission from deforestation and forest Degradation in Developing countries) projects for the region started in 2008 [17]. By this time, Brazil was close to reaching the goal of reducing deforestation by 80% until 2020 (green, dashed line in Figure 1B) compared to the 1996–2005 period (black line). That goal was set in 2009 during the United Nations Framework Convention on Climate Change (UNFCCC) held in Copenhagen, Denmark [18]. The trend, however, inverted as indicated by the steady growth of the red line in Figure 1B. The inflexion is linked to the Federal Law n. 12.727/2012 [19], that relaxed, to some extent, forest conservation. As of 2019, deforestation in Pará State alone was higher than the target value set in 2009 for the whole Brazilian Amazon.

Figure 2 shows the relationship between land use and land cover changes, and forest fire in the Brazilian Amazon, as proposed by [5,6]. Road construction facilitates forest access, accelerating deforestation and selective logging, and lowering the resilience of surrounding forests to fire [20–23]. Deforestation raises the number of forest edges, increasing the susceptibility of forests to fires [24–27]. Deforestation raises the number of forest edges, increasing the susceptibility of forests to fires [24,26]. Selective logging degrades forest, reduces canopy and soil moisture, and increases canopy temperature and tree mortality, intensifying fire outbreaks [22,28,29]. The cycle grows in a spiral configuration: forest fires and smoke emissions reduce rainfall, particularly in the dry season, as a result of El Niño events [24,30–35]; previously burned areas are more prone to recurrence; changes in the global and local climate, along with land use intensification, contribute to increasing the level of forest degradation [28,35–41]; most significant changes in forest canopy density take place in regions close to the forest edges [16,22,35,42], and land management fires can penetrate the standing degraded forests, as demonstrated by others works [21,43,44].
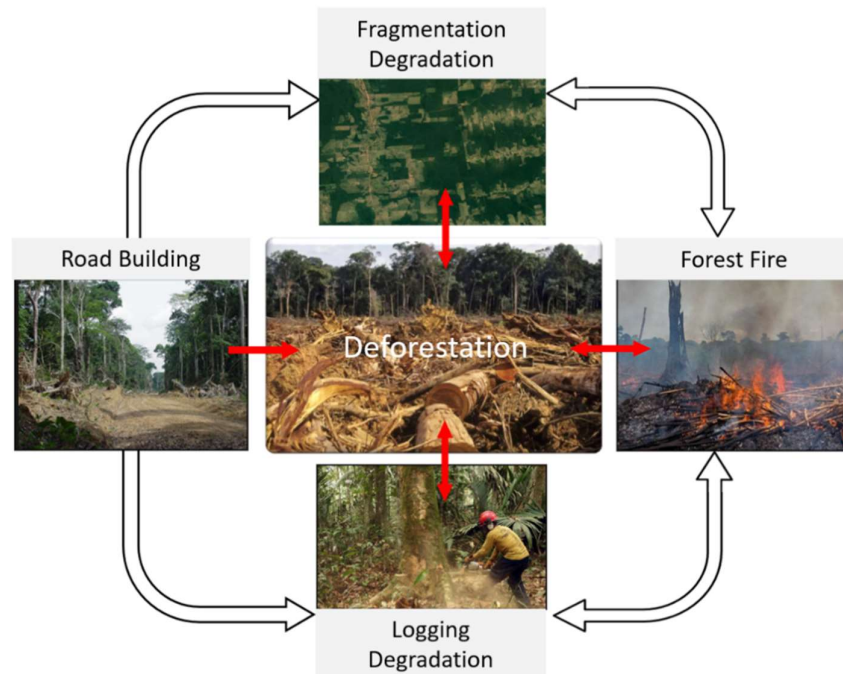
Figure 2. Relationship between land use and land cover changes and fire occurrences. Sources: [5,6].

Several in-situ measurements of the slash-and-burn forest clearing practices have been conducted to infer greenhouse gas (GHG) emission [45–49]. Figure 3 shows the main steps of the slash-and-burn practices observed in the Brazilian Amazon rainforest. By the end of the rainy season, the forest is clear-cut (Figure 3A) and left in the terrain to dry until the peak of the dry season (Figure 3B), after which the fire is set. The burning period typically extends from July to October. The initial fire consumes the duff-layer, small branches, and leaves, while most of the massive trunks remain in the terrain (Figure 3C). Finally, the remaining scorched logs are stockpiled and burned along the coming years until the terrain becomes dominantly bare soil (Figure 3D). Fire may penetrate the standing forest if moisture favours flame propagation through the understory vegetation [42–44]. Forest degradation increases after successive fires, observed by the combustion of growing, small trees along dry seasons. The less resilient forest also favours significant fire recurrences over the years. Fire is used mainly for land management, mostly for clearing the terrain after the slash-and-burn deforestation for subsequent maintenance of deforested areas [50,51].

GHG emissions from deforestation in the Brazilian Amazon are also of great concern considering that it generally accounts for more than 200 t ha^{-1} of CO_2 after the clear-cut occupation [44,49,52]. These authors also observed that other gases such as CO, CH_4, and non-methane hydrocarbons and particulates are also emitted in large quantities.
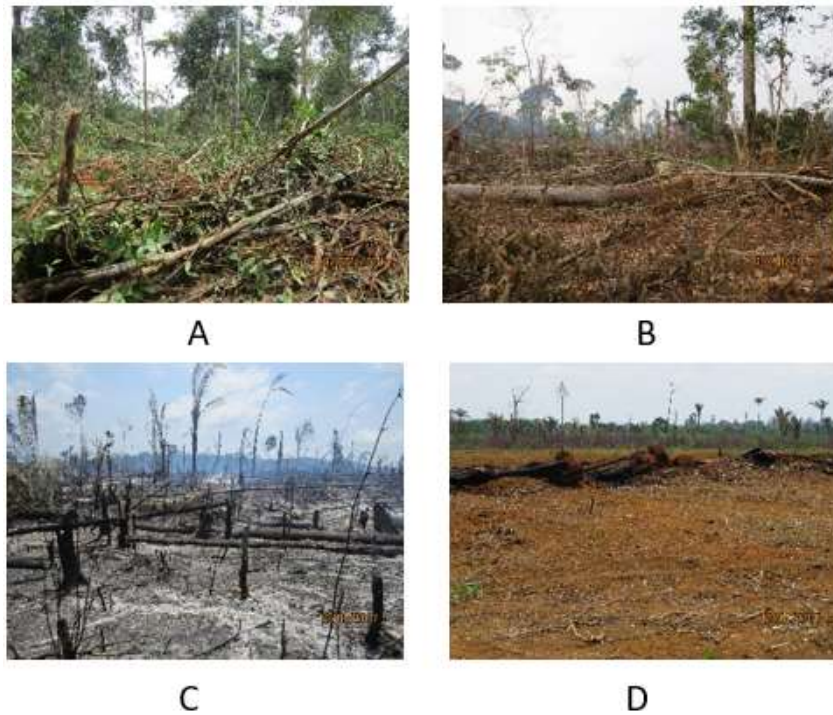
Figure 3. Main stages of the clear-cut processes of a forest clearing in the Brazilian Amazon. (A) clear-cut during the wet season or end of the wet season; (B) trunks and branches left in the terrain for drying; (C) burning activity during the dry season; and (D) bare soil prepared for pasture or crop plantation. (Photos: E. Sano).

Considering the actual rate of increase of human occupation towards the Brazilian Amazon rainforest, this paper addresses the relationship between forest loss, the occurrence of fire, and primary GHG emissions. We relied on annual reports published by INPE, for the period 2006-2019. The data were used to correlate fire events in a specific area (Novo Progresso municipality) and in a regional area (Pará State) both located in the Deforestation Arch of the Brazilian Amazon. Fire outbreaks inside the primary forest were also investigated to assess ecosystem degradation. The work also presents the amount of GHG originated by the forest clearing process along the Brazilian rainforest in 2019. The period of 2007–2019 was selected for this study, as it has sharp decay on deforestation rates followed by the steady growth on human occupation after 2012, as depicted in Figure 1.

2. Materials and Methods

2.1. Novo Progresso region

Pará State encompasses an area of 1,246,000 km², equivalent to the total area occupied by Germany, France, the United Kingdom, and Italy altogether. The Novo Progresso region, located in the southwest of the Pará State (Figure 4), covers 36,800 km². Most of the deforestation in the Novo Progresso region is found along the BR-163 highway, crossing the region in the North/South direction.
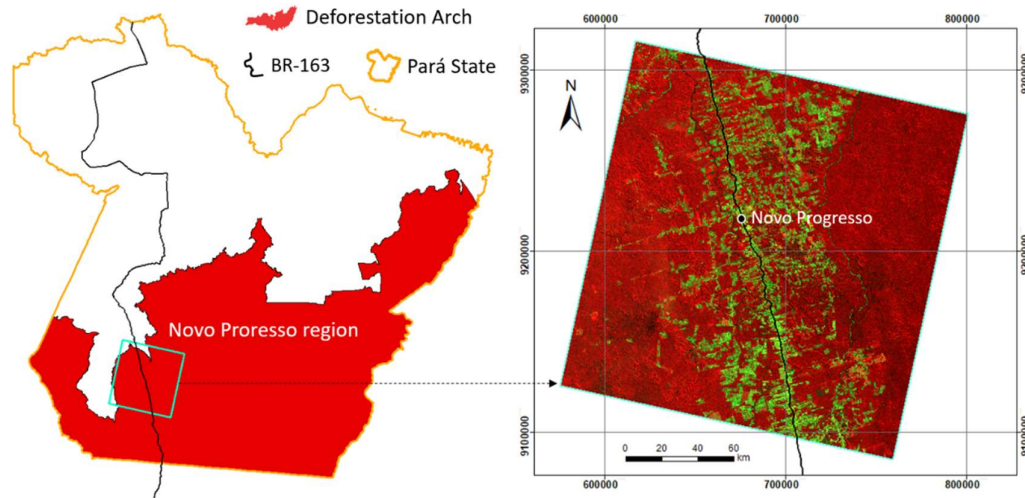
Figure 4. Location of the Novo Progresso region, southwest of the Pará State. RGB false-color composite of bands 5, 4, and 3 of Landsat 8 satellite images [53].

2.2. Datasets

The datasets of deforestation and fire hotspots were produced by the INPE´s Amazon Deforestation Satellite Monitoring Program (PRODES) and the Forest Fire Program, respectively. PRODES provides the annual rates of clear-cut deforested areas larger than 6.25 hectares over the Brazilian Amazon [54]. The system makes use of moderate spatial resolution (10-100 m), optical data, mostly from the dry season, obtained by Landsat 8 (30-m spatial resolution and 16-day revisit time), China-Brazil Earth Resources Satellite (CBERS-4) (20-m spatial resolution and 26-day revisit time), and Sentinel-2 (10-m spatial resolution and 5-day revisit time) satellites.

The near real-time fire detection data, provided by the Forest Fire Program (*Programa Queimadas*) [54], are based on thermal sensors onboard several sun-synchronous and geostationary satellites, namely:

- MODerate Resolution Imaging Spectroradiometer (MODIS) sensor onboard Aqua and Terra platforms;
- AVHRR (Advanced Very High Resolution Radiometer) sensor onboard NOAA satellite;
- AVHRR3 (Advanced Very High Resolution Radiometer) and Infrared Atmospheric Sounder Interferometer (IASI) sensors onboard MetOp satellite;
- Visible Infrared Imaging Radiometer Suite (VIIRS) sensor onboard Suomi National Polar-orbiting Partnership (NPP) satellite;
- Advanced Baseline Imager (ABI) sensor, onboard GOES-R satellite; and
- Spinning Enhanced Visible and Infrared Imager (SEVIRI) sensor onboard Meteosat Second Generation (MSG) satellite.

Daily fire hotspot monitoring is performed by the MODIS sensor (Collection 6), onboard the Aqua and Terra platforms [54–56]. The detection of fire hotspots by INPE through satellite images is carried out by using well-known techniques [57–60] that is by comparison of brightness temperatures measured in the middle infrared (MIR) band (around 4 μm) with that of the measured thermal infrared (TIR) band (around 11 μm). Thermal anomalies are identified when the difference in the brightness temperature measured in these two spectral bands is higher than a given threshold, i.e. when the temperature from MIR being much higher than that of TIR. Hantson et al. [61] investigated the strengths and weaknesses of hotspots detected by MODIS to characterize fire occurrence in many different ecosystems. For the Brazilian Amazon, they reported less than 2.1% of commissioning error, 80% confidence interval between hotspot detection (MODIS) and burned area (Landsat). The coefficient of determination between the annual number of hotspots and burned areas for the Amazon was $R^2 = 0.95$.

2.2. Methodology

2.2.1. Deforestation and fire hotspots

In the southwest region of Pará State, typical raining season is from November to May and typical dry season is from June to October [62]. INPE´s deforestation mapping starts on 1st August of the previous year until 31st July of the current year. In this paper, this period is referred as PY (PRODES Year). In PRODES, the processing time is quite long to account for the required level of confidence (>90%) and the size of the region (deforestation arch). Deforestation reports are generally published four months after the end of the mapping period.

Fire occurrences within the forest and deforested areas covered for the same reference period (2007–2019) to evaluate their strength of relationship with deforestation. To avoid misinterpretations, the reference year for the hotspots follows that of deforestation. Most planned fires, however, take place in the mid/end of the dry season (August-September), for higher combustion efficiency. The first fires consume about 50% of the recently slashed biomass. The scorched biomass is then stockpiled and burnt in the following years to complete the land clearing process. The newly deforested areas reported for a given PY show intense fire activities in the first months of PY+1 (August-September), but fire hotspots are likely to appear at that pre-burnt area for the next PRODES years (PY+2, PY+3, PY+4), though at lesser intensity when compared to the first burn. Throughout the work, fire scars, hotspots, and fire outbreaks are mentioned indiscriminately and are considered as indicative of the spatial and temporal burned areas.

Figure 5 illustrates, for a given year, the accumulative location of detected fire hotspots inside the forest shown as red dots, and in the deforested areas, indicated by blue dots. Hotspots' location accuracy is ±500 m. Due to positioning uncertainty, the fire hotspots reported at a distance higher than 500 meters (buffer zone) from the edge of deforested areas were considered to take place at the standing forest. The boundaries of deforested areas were updated annually. Therefore, the buffer zone of 500 m was updated accordingly. Figure 5 shows the consolidated data of forest and non-forest as reported by INPE, corresponding to the actual status of the region by 31st July 2019 (PY2018-2019). The hotspots in Figure 5 give the location of their incidences at any time during the period of 1st August, 2018 to 31st July, 2019. The majority of fire hotspots would appear in the dry season of 2018, from July to October for which clear-cut had occurred at the first quarter of 2018 (PY2017-2018).
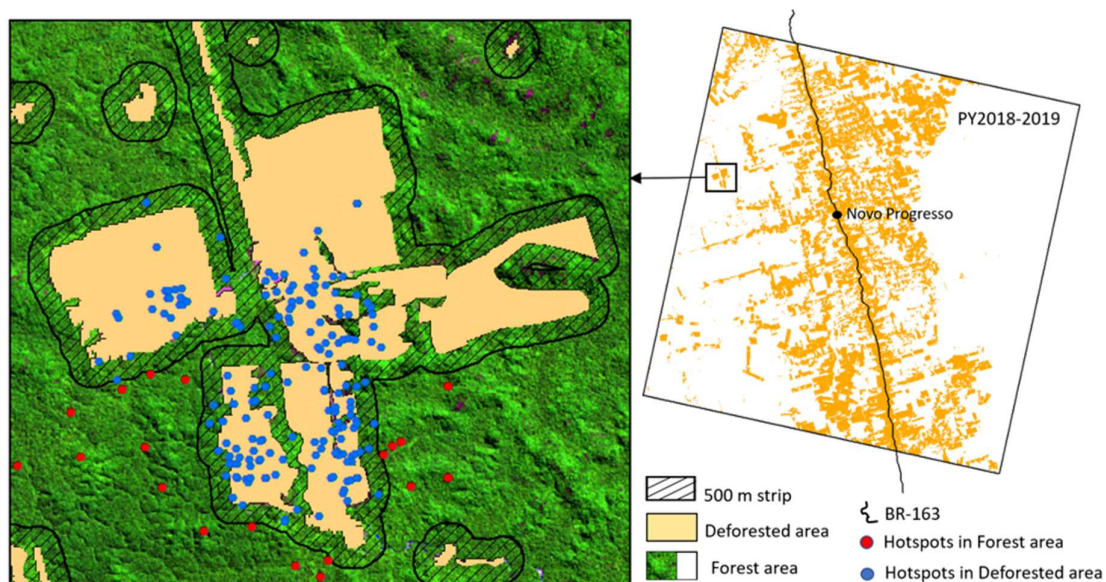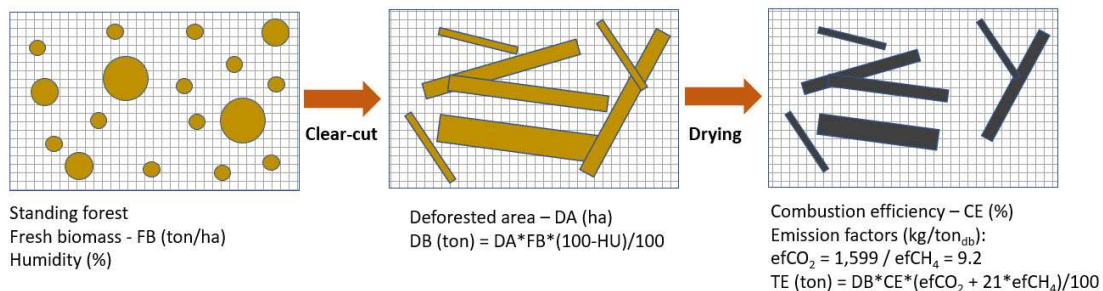

Figure 5. Examples of deforested areas (yellow and striped polygons), forest (green and white areas), fire hotspots in the forest areas (red dots), fire hotspots in the deforested areas (blue dots), and deforestation dynamics example (dotted square) in the Novo Progresso region.

It is important to highlight that the healthy undisturbed forest does not sustain large fires in the Brazilian Amazon, due to the high levels of humidity, even in the dry season. Fire occurrences in the humid tropical forest are observed in dead trees and along the duff-layer. The understory vegetation may propagate flame in the surroundings of large cleared areas (degraded edges of forests) in combination with an intense dry season. Flame propagation through the understory vegetation is too weak to be captured by satellite sensors. Therefore, the fire hotspots inside the intact forest may be due to the flaming of large naturally dead trees or along an open forest trail where small slashed trees has the ability to sustain the fire. Selective logging also degrades the area around the large falling trees, thus making the vicinity prone to propagate flame. Fire occurrences inside the standing forest are restricted to degraded forest caused by any of the previously discussed event or their combined effects.

This study deals with deforestation and the use of fire for land clearing. Fire hotspots may also occur in nearby degraded areas, such as dead trees, in the vicinity of extracted logs and trails. Total GHG emissions for the Amazon was limited to the burn of the newly deforested area corrected by the average regrowth of secondary forest throughout.

2.2.2. Greenhouse gas emissions

Amazon GHG emissions from slash-and-burn practices can be estimated based on in-situ measurements of forest clearing fire experiments [49,52]. Figure 6 explains the GHG estimation model. Emissions are calculated based on the amount of burned dry biomass, combustion efficiency and the emission factors for each gas. The dry weight of biomass (ton) is estimated from the local fresh biomass correlation (ton/ha), its humidity (%), and the a Fire occurrences in the humid tropical forest mount of deforested area (ha). For the Novo Progresso region, we used the data obtained [49] from two different sites in the Alta Floresta municipality, which is less than 500 km from the Novo Progresso region. For the Pará State, the fresh biomass (ton/ha) was calculated by averaging the estimates of Alta Floresta in addition to that of the calculated biomass for Manaus [46,47,49,52]. For the whole forest, the average fresh biomass (ton/ha) included the values from the Pará State and those measurements from municipalities of Cruzeiro do Sul and Rio Branco, both in Acre State. More detailed information about the methodology of the GHG emissions and estimates can be found in Carvalho Jr. et al. [49] and Soares Neto et al. [52].

Standing forest
Fresh biomass - FB (ton/ha)
Humidity (%)

Deforested area – DA (ha)
DB (ton) = DA*FB*(100-HU)/100

Combustion efficiency – CE (%)
Emission factors (kg/ton_{db}):
$efCO_2$ = 1,599 / $efCH_4$ = 9.2
TE (ton) = DB*CE*($efCO_2$ + 21*$efCH_4$)/100

Figure 6. Procedure of the estimation of the GHG emission. HU = humidity; DB = dry biomass, TE = total emission.

Soares Neto et al. [52] reported combustion efficiencies of about 50% and fresh biomass humidity of 42%, prior to clear-cut. Table 1 summarizes the relevant data for emission estimates from slash-and-burn activities in the Brazilian Amazon rainforest.

Table 1. Basic data for gas emissions estimate. Source: [49,52].

Parameter	Reference value	Reference area
Fresh biomass (ton/ha)	512	Novo Progresso
Fresh biomass (ton/ha)	570	Pará State
Fresh biomass (ton/ha)	580	Brazilian Amazon
Emission factor CH_4 (kg/ton$_{db}$)[*]	9.2	Brazilian Amazon
Emission factor CO (kg/ton$_{db}$)	111.3	Brazilian Amazon
Emission factor CO_2 (kg/ton$_{db}$)	1599	Brazilian Amazon
Emission factor NMHC (kg/ton$_{db}$)	5.57	Brazilian Amazon
Emission factor $PM_{2.5}$ (kg/ton$_{db}$)	4.84	Brazilian Amazon
Fresh biomass humidity (%)	42	Brazilian Amazon
Combustion efficiency (%)	50	Brazilian Amazon

[*] db refers to mass of dry biomass burned.

3. Results and Discussion

3.1. Fire hotspots in the Novo Progresso region

Table 2 reports the statistics about the fire hotspot occurrences inside the deforested and forest areas in the Novo Progresso region. We found a total of 11,769 fire hotspots in PY2006-2007, with 9,702 located in deforested areas (corresponding to 5,230.90 km²) and 2,067 in forest areas (corresponding to an area of 31,574.50 km²). In PY2018-2019, the total fire outbreaks detected from 1st August 2018 to 31st July 2019 was 39,384, from which 37,236 over 8,481.80 km² of deforested area, and 2,148 over 28,323.70 km² of intact forest.

Table 2. Total annual fire hotspots distribution in the Novo Progresso region. Deforested and forest areas and fire hotspots are reported from PY2006-2007 until PY2018-2019 in the Novo Progresso region. PY = PRODES year.

| PY	Forest Area (km²)	Accumulated Deforested Area (km²)	Annual Deforested Area (km²)	Hotspots in Forest	Hotspots in Deforested Area	Total Annual Hotspots
2006-2007	31,574.5	5,230.9		2,067	9,702	11,769
2007-2008	31,153.6	5,651.9	421.0	2,012	9,870	11,882
2008-2009	30,543.9	6,261.5	609.6	1,345	7,753	9,098
2009-2010	30,406.7	6,398.7	137.2	1,035	5,060	6,095
2010-2011	30,281.5	6,524.0	125.3	1,675	9,573	11,248
2011-2012	30,096.5	6,708.9	184.9	572	3,621	4,193
2012-2013	29,704.1	7,101.3	392.4	4,536	36,350	40,886
2013-2014	29,437.9	7,367.6	266.3	457	10,186	10,643
2014-2015	29,200.6	7,604.8	237.3	3,243	34,817	38,060
2015-2016	29,021.9	7,783.5	178.7	2,085	32,196	34,281
2016-2017	28,938.4	7,867.1	83.6	1,212	19,572	20,784
2017-2018	28,655.2	8,150.3	283.2	4,338	42,723	47,061
2018-2019	28,323.7	8,481.8	331.5	2,148	37,236	39,384

Figure 7 shows the variation of total fire outbreaks relative to PY2006-2007 and accumulated deforestation in the Novo Progresso region. From PY2006-2007 to PY2018-2019, deforested areas increased by 8.8%, with a positive correlation of 0.72 with total detected fire hotspots for the same area. The variation of hotspots was stable from PY2006-2007 to PY2011-2012 and increased from PY2012-2013 to PY2018-2019. Deforested areas increased from 4.0% of the period PY2006-2007 – PY2011-2012 to 4.8% of the period PY2012-2013 – PY2018-2019. The average of fire outbreaks was 9047 against 33,014 from PY2012-2013 to PY2018-2019, a three-fold increase.

In tropical forests, deforestation and land management practices are usually associated with the use of fire [4–12]. In the Novo Progresso region, studies carried on burned area detection, with MODIS time series for the period 2000–2014, identified more than 70% of fire events over deforested areas [63]. The sharp increase in fire hotspots for the period of PY2012-2013 until PY2018-2019 may be related to the current Brazilian Forest Code [19]. This law states that farmers located in the Brazilian Amazon need to maintain 80% of their land with native vegetation if located in forestlands or 30% if located in non-forestlands. However, the law amnestied 58% of the required restoration areas deforested illegally before 2008 [64]. Therefore, the increase in total fire hotspots from 2013 may be associated with the relaxation from the prevailing law.
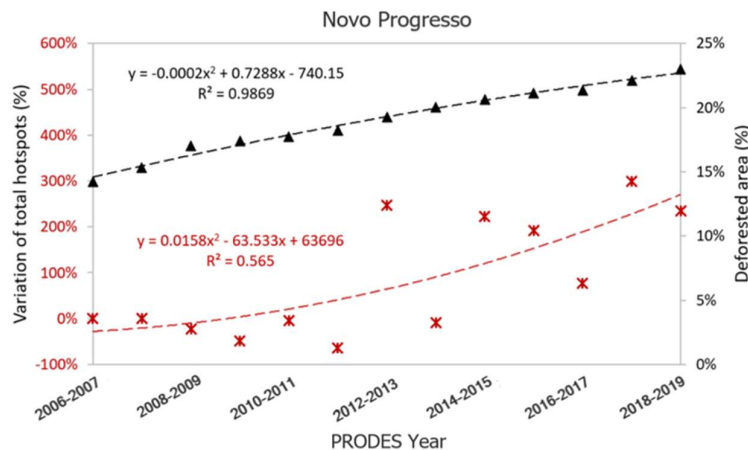
Figure 7. Variation of the total fire hotspots (red) relative to the year PY2006-2007 and accumulated deforestation area (black) in the Novo Progresso region.

Figure 8 exemplifies the dynamics of deforestation occurred in the Novo Progresso region. Deforested areas, shown in yellow, are accumulative over the period under investigation. The newly deforested area shown in the right down corner of PY2012-2013 was subjected to intense fire activity. The clear-cut process and fire occurred in the same PRODES year of 2012-2013. For that area, a significant number of fire outbreaks were detected in PY2012-2013, PY2013-2014, and PY2014-2015. Some hotspots were detected in PY2016-2017 and PY2018-2019. The less intense fire hotspots after PY2016-2017 is an indication that the area was almost free of original forest residues.
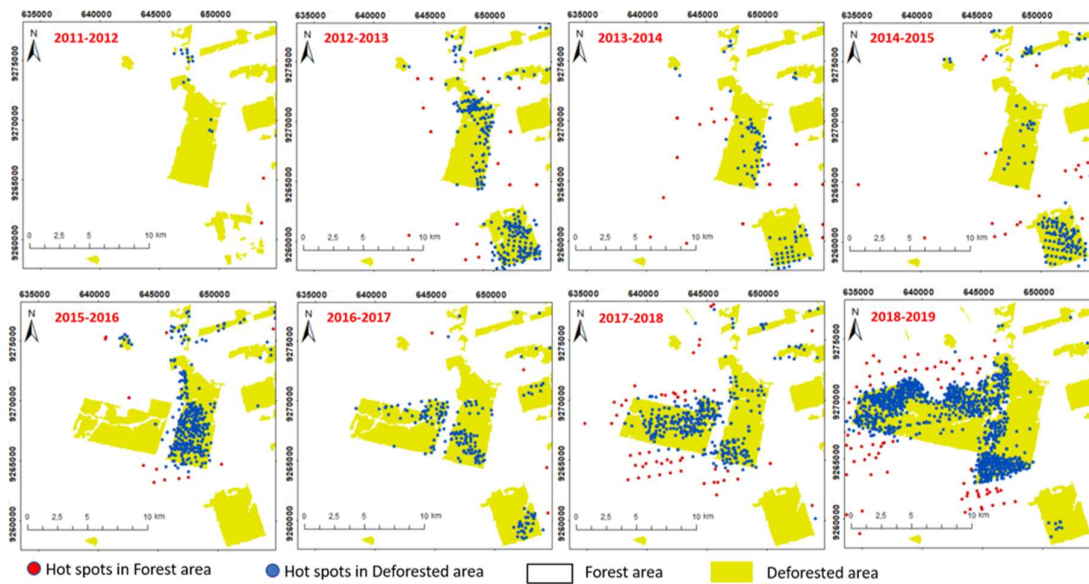
Figure 8. Deforestation dynamics from PY2011-2012 to PY2018-2019 in a portion of the Novo Progresso region, showing the evolution of hotspots related to deforestation in deforested (blue dots) and forested (red dots) areas.

The fire hotspots over recently deforested areas (clear-cut) are man-induced, as a rapid and cheap means to clear the area (slash-and-burn) that can be observed by comparing Figure 3B and 3C. Eventually, the fire set to clean a given deforested area may propagate fire on nearby pasture, or on some crop area or even through the understory of a standing forest, by accident. Fire occurrences inside consolidated occupied areas may suggest land management, as shown in the large deforested area in PY2012-2013. For this area, the high density of hotspots was detected in PY2015–2016 and decayed in the following two years. The high concentration of fire outbreaks in deforested areas is caused by either the combustion of old pre-carbonized trunks that were not burned in the previous years or due to the burning of pasture, caused by an advance of the fire front from the deforested area or even land management.

The same land claiming dynamics occurred at the newly deforested central area of PY2015–2016, as shown in Figure 8. For that area, fire activities started in PY2016–2017, several months after the clear-cut process. Fire intensity increases sharply thereafter, as it can be seen in PY2017–2018. Burning activities were also observed in PY2018–2019, though with less intensity. The slash-and-burn approach for clearing the forest is even more evident by observing PY2018-2019 in Figure 8. The strong overlapping of deforestation and fire occurrences, shown by the large concentration of hotspots, indicates that the clear-cut took place after 31st July 2018, and the slashed biomass was most likely burnt during the dry season of the same year (2018). The method seemed different from the previous years since forest clearing usually takes place in the rainy season, i.e., in the first quarter of PY, and the fire activity starts in the third quarter of the same year but reported as PY+1. Such forest clearing processes, also reported by different researchers [5,6,8,11,12,27], confirm the cycle depicted in Figure 2. It begins with the extraction of high commercial value trees (selective logging), followed by the removal of smaller trees and by the clear-cutting of remaining trees and shrubs, producing deforestation in the middle of the forest. As regards to the large scorched trunks, the clearing process

may extend for about five to six years until the remaining logs that were stockpiled had been combusted to completion.

The occurrence of fire inside deforested areas can be observed in Figure 9. In PY2006–2007, the deforested area corresponded to 14.2% of the total Novo Progresso region. For the considered period, there was a steady increase in deforestation. By PY2018-2019, the deforested area accounted for 23.0%, an increase of 8.8% in land cleaning, which corresponds to an area of 3,250 km². In PY2006-2007, there were 11,769 occurrences of fire hotspots in the Novo Progresso region, of which 82.4% were in deforested areas. In PY2018-2019, this value reached 94.5%, an increase of 12.1%. Fire outbreaks in deforested areas indicate the systematic use of fire as a means for new land clearing and land management practices.

The highest annual rate of deforestation occurred in PY2008-2009 (609.6 km²) and the lowest in PY2016-2017 (83.5 km²) (Table 2). After PY2008-2009, a deforestation peak occurred in PY2012-2013 (392.4 km²), followed by the periods of PY2017-2018 and PY2018-2019 when deforestation rates raised again. Fire hotspots, though, increased at higher rates than deforestation, the curve fitting of fire outbreaks indicates a somehow steady increase of fire occurrences for the studied period. The average number of hotspots was 7,597 from PY2006-2007 to PY2011-2012 and 30,440 from PY2012-2013 to PY2018-2019, four times higher than the previous period.
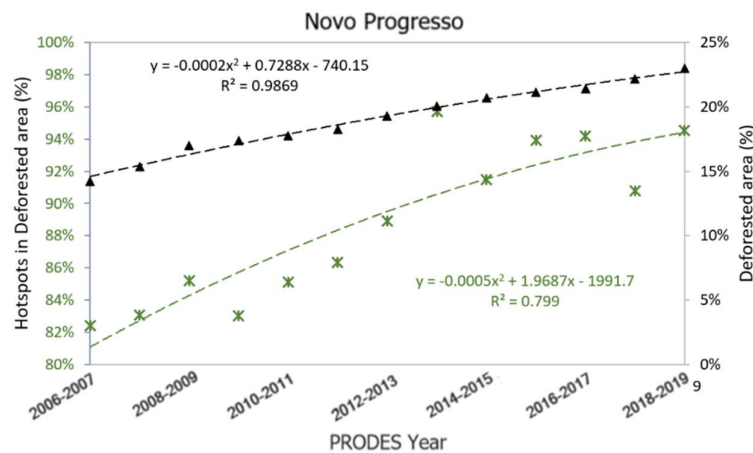
Figure 9. Temporal analysis of fire hotspots occurrence in the deforested areas (grey) and the relative increase of deforestation (black) in the Novo Progresso region.

Figure 10 shows the number of fire hotspots detected inside the standing forest for PY2018-2019 as a function of distance from the edge of the deforested area. As can be seen, a significant incidence of fire outbreaks occurred in the first 800 m from the margins and extended up to 1200 m. The same behavior was also observed for the previous years. Other researchers had already recognized a more significant frequency of fires within forest areas and in the vicinity of the deforested areas [4–6,16,43,44,50]. In particular, the hotspot occurrences behavior agrees with the data reported by some researchers [40,44]. The increase of fires around the edges of deforested areas enhances the forest degradation along the edges. The decrease in forest resilience to fire makes it more susceptible to sustain biomass combustion due to the reduction in near-the-edge forest humidity. Periods of severe drought combined with an intense slash-and-burn activities favour the outbreaks of fires in standing degraded forests [65].

The research carried out by Matricardi et al. [66], during the period 1992 to 2014, revealed that forest degradation in the Brazilian Amazon had surpassed deforestation. They attributed 40% of the whole Amazon forest was degraded by intensive logging and understory fires, and remaining 60% through edges and isolated forest fragmentation.
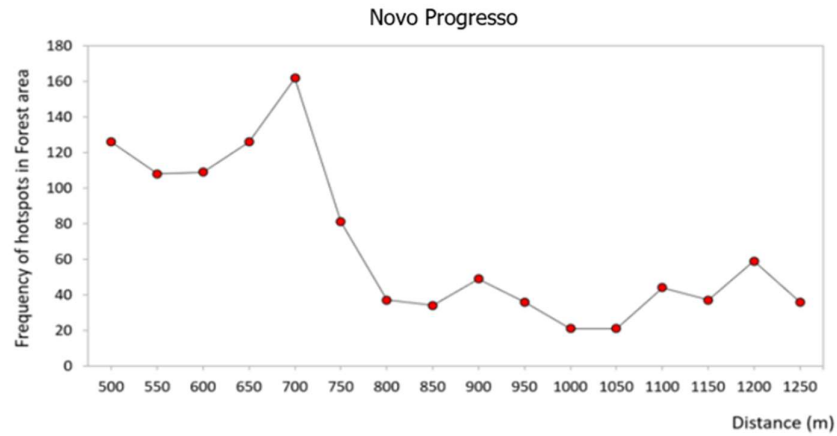
Figure 10. Number of fire hotspots in the forest area, for the PY2018-2019, identified according to their distance from the borders of the deforested areas in the Novo Progresso region.

3.2. Fire hotspots and deforestation in the Pará State

In recent years, Pará State has faced high deforestation rates in the Brazilian Amazon. Table 3 shows the total occurrence of annual fire hotspots, the accumulated deforested areas, and the annual deforested area in this state. A total of 146,863 fire hotspots were detected in PY2006-2007 and 351,001 fire hotspots in PY2018-2019. In PY2006-2007, there was an accumulated deforested area equivalent to 9.35%. From PY2006-2007 to PY2018-2019, the deforested area reached 12.30%, a 2.95% increase in deforestation for the specified period and area of 42,350 km^2. Fire occurrences, however, increased at a rate higher than deforestation, which also indicates forest degradation [4–6,29,65,66].

Table 3. Distribution of the total annual fire hotspots, accumulated deforested area (%), and annual deforested area (km^2) in the Pará State, analyzed from July 2007 to December 2019.

PY	Total Annual Fire Hotspots	Accumulated Deforested area (%)	Annual Deforested Area (km^2)
2006-2007	146,863	9.35	5,526
2007-2008	202,922	9.80	5,607
2008-2009	119,234	10.14	4,281
2009-2010	113,174	10.44	3,770
2010-2011	174,394	10.69	3,008
2011-2012	80,401	10.83	1,741
2012-2013	372,391	11.01	2,346
2013-2014	181,458	11.17	1,887
2014-2015	324,024	11.34	2,153
2015-2016	560,591	11.58	2,992
2016-2017	276,283	11.77	2,433

| 2017-2018 | 692,498 | 11.99 | 2,744 |
| 2018-2019 | 351,001 | 12.30 | 3,862 |

Source: Fire hotspots from the *Projeto Queimadas* and deforestation from PRODES project produced by the National Institute for Space Research (INPE).

Figure 11 shows the variation of total fire hotspots from PY2007 to PY2019 along with the accumulated deforestation area in the Pará State. There was a positive correlation of 0.66 between total hotspots and deforested areas. It can be observed that the variation of total hotspots was stable from PY2006-2007 to PY2011-2012 and increased from PY2012-2013 to PY2018-2019. Similar trends were observed for the smaller area (Figure 9). There is an expectation that the local and regional deforestation practices also apply for the entire deforestation arch.
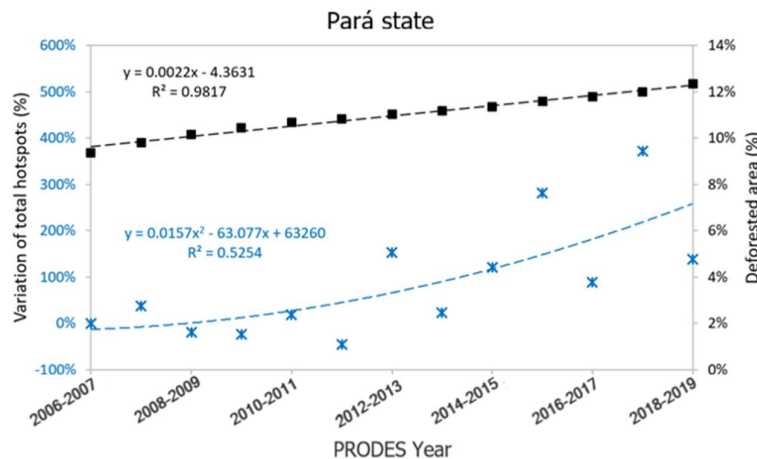
Figure 11. Variation of the total fire hotspots (blue) relative to the year PY2006-2007 and accumulated deforestation area (black) in the Pará State.

3.3. Gas and particulate emissions

Total gas and particulate emissions as a function of the burned area was calculated and summarized in Table 4. These data represent the emissions exclusively with the combustion of biomass from slash-and-burn activities. The efficiency of the first fire was about 50%. It did not include small fires that may take place in the degraded standing forest, pasture, or crop remaining over the bare soil. Also, the emissions are solely from the first fire of the newly slashed area. Over the years, after the initial large fire, stockpiled scorched biomass, i.e., the remaining 50%, is subjected to successive burns, ultimately approaching 100% combustion efficiency for that newly deforested area. Total CO_2 emissions accounted for the methane that is converted into an equivalent amount of CO_2, considering its relative radiative forcing, plus the emissions of the CO_2 itself, as shown in Figure 6.

Table 4. Gas emission estimates as for PY2019 slash-and-burn activities in the Brazilian Amazon.

Parameter (units)	Novo Progresso region	Pará State	Brazilian Amazon
Deforested area (ha)	33.15E+03	446.3E+03	1.0897E+06
Fresh biomass (ton/ha)	512	569.7	580.4
Total Biomass (ton)	1.697E+07	2.542E+08	6.324E+08
CH_4 emitted (Mton)	0.047	0.67	1.7
CO_2 emitted (Mton)	7.86	109.2	293.3

Total CO_2 (Mton)	8.81	132.1	328.7
CO emitted (Mton)	0.55	8.3	20.41
NMHC emitted (Mton)	0.027	0.41	1.02
$PM_{2.5}$ emitted (Mton)	0.024	0.36	0.89

A small region such as Novo Progresso emitted about 8.81 megatons (Mton) of CO_2 over 331 km^2 of land approximately for the year PY2018-2019. For comparison, the carbon emission of Abruzzo region (Italy), with 1.30 million inhabitants, is 11.1 Mton for the year 2006 [67]. These data are even more alarming when we consider the emissions after deforestation practices in the Pará State and the Brazilian Amazon, accounting for 132.1 and 328.7 Mton of CO_2 released to the atmosphere, respectively, in the PY2018-2019. Other emissions are also of great concern in local and regional scales, notably, particulates of diameter less than 2.5 mm. Local, regional, and total emissions were about 0.027, 0.41, and 0.89 Mton, respectively. The same applies to CO emissions, accounting for 0.55, 8.3, and 20.41 Mton in Novo Progresso, Pará State, and Brazilian Amazon, respectively.

After the year 2000, high deforestation rates were observed in the period of 2002 to 2004, with an average of 24,939 km^2. In this time span, the lowest deforestation occurred in 2012, equivalent to 4,561 km^2 following the voluntary REDD+ projects starting year [17]. Applying the same emission factors and other relevant data from Table 1, the total CO_2 emissions for the period 2002–2004 and in 2012 were 752.3 Mton and 137.6 Mton on average, respectively. The CO_2 emissions from 2019 are, therefore, 2.38 times higher than the minimum (2012) and 2.29 times smaller than the maximum (2002–2004). Emissions were estimated based on the deforested area. The results were not corrected for a possible offset from forest regrowth. According to Smith et al. [68], the yearly increase in secondary forest extent in the Brazilian Amazon was about 8.61 ± 10.96%, offsetting GHG emissions from newly slash-and-burned areas by 10.29 ± 6.8%. Taking this scenerio into consideration, the net emissions from fires, for the year 2019 was 295 Mton of CO_2 for the Brazilian Amazon.

In Brazil, the total CO_2 emissions related to deforestation practices of newly slashed areas in the Brazilian Amazon are higher than those from transport, electricity and heat, manufacturing, industry, buildings, aviation, and shipping sectors of the Brazilian economy. The emissions from deforestation of the Amazon rainforest in Brazil is next to the agricultural sector.

A rough estimate of burned biomass on wide areas can be carried out using geostationary satellite sensor data starting from the computation of the fire radiative power, which is the power radiated by the fire. By integrating this quantity over time, it is possible to estimate the radiative fire energy and the burned biomass, and then the emissions in the atmosphere if the coefficients providing the burning efficiency of vegetation affected by the fire are available [69]. It will be the subject of a forthcoming paper.

5. Conclusions

This work showed a strong correlation between the occurrence of fire in the newly deforested area in the municipality of Novo Progresso following the local slash-and-burn practices. The same trends were also observed for the Pará State, suggesting a common practice along with the Deforestation Arch. The study indicated positive correlations of 0.72 and 0.66 between deforestation and fire occurrences in local and regional scales, respectively. The use of fire as a rapid means for forest clearing was evident for the PY2018-2019, which showed a strong overlapping of slash-and-burn activities in a brief period of time. A large number of fire occurrences inside the forest in the near recent deforested areas is a result of ecosystem degradation, which is more prone to future fire events. The area of old-growth forest, negatively influenced by nearby slash-and-burn practices, are a fraction of the deforested area, thus enlarging forest degradation. The steady increase in deforestation after the PY2011-2012 is a worldwide concern because of the loss of intact forest and

the massive greenhouse gases emissions, from the slash-and-burn practices, accounting about 295 million tons of CO_2, for the PY2018-2019 alone.

References

1. Aragão, L.E.O.C.; Poulter, B.; Barlow, J.B.; Anderson, L.O.; Malhi, Y.; Saatchi, S.; Phillips, O.L.; Gloor, E. Environmental change and the carbon balance of Amazonian forests. *Biol. Rev.*, **2014**, *89*, 913–931, 2014. DOI: 10.1111/brv.12088.

2. FAO. UM-REDD Programme. Available online: http://www.un-redd.org/how-we-work (accessed on 31 August, 2020).

3. Bustamante, M.M.; Roitman, I.; Aide, T.M.; Alencar, A.; Anderson, L.O.; et al. Toward an integrated monitoring framework to assess the effects of tropical forest degradation and recovery on carbon stocks and biodiversity. *Glob. Change Biol.*, **2016**, *22*, 92–109. DOI: 10.1111/gcb.13087.

4. Nepstad, D.C.; Veríssimo, A.; Alencar, A.; Nobre, C.; Lima, E.; Lefebvre, P.; Schlesinger, P.; Potter, C.; Moutinho, P.; Mendoza, E.; Cochrane, M. Brooks, V. Large-scale impoverishment of Amazonian forests by logging and fire. *Nature*, **1999**, *398*, 505–508. DOI: 10.1038/19066.

5. Nepstad, D.; Carvalho, G.; Barros, A.C.; Alencar, A.; Capobianco, J.P.; Bishop, J.; Moutinho, P.; Lefebvre, P.; Silva Jr., U.L.; Prins, E. Road paving, fire regime feedbacks, and the future of Amazon forests. *For. Ecol. Manag.*, **2001**, *154*, 395–407. DOI: 10.1016/S0378-1127(01)00511-4.

6. Cochrane, M.A. Fire science for rainforests. *Nature*, **2003**, *421*, 913–919. DOI: 10.1038/nature01437.

7. Bowman, M.S.; Soares-Filho, B.S.; Merry, F.D.; Nepstad, D.C.; Rodrigues, H.; Almeida, O.T. Persistence of cattle ranching in the Brazilian Amazon: A spatial analysis of the rationale for beef production. *Land Use Policy*, **2012**, *29*, 558–568. DOI: 10.1016/j.landusepol.2011.09.009, 2012.

8. Domingues, M.S.; Bermann, C. O arco de desflorestamento na Amazônia: da pecuária à soja. *Ambient. Soc.*, **2012**, *15*, 1–22. DOI: 10.1590/S1414-753X2012000200002.

9. Kastens, J.H.; Brown, J.C.; Coutinho, A.C.; Bishop, C.R.; Esquerdo, J.C.D.M. Soy moratorium impacts on soybean and deforestation dynamics in Mato Grosso, Brazil. *PLoS One*, **2017**, 12, e0176168. DOI: 10.1371/journal.pone.0176168.

10. Yanai, A.M.; Nogueira, E.M.; Graça, P.M.L.A.; Fearnside, P.M. Deforestation and carbon stock loss in Brazil's Amazonian settlements. *Environ. Manag.* **2017**, *59*, 393–409. DOI: 10.1007/s00267-016-0783-2.

11. Farias, M.H.C.S.; Beltrão, N.E.S.; Cordeiro, Y.E.M.; Santos, C.A. Impact of rural settlements on the deforestation of the Amazon. *Mercator*, **2018**, *17*, e17009. DOI: 10.4215/rm2018.e17009.

12. Yanai, A.M.; Graça, P.M.L.A; Escada, M.I.S.; Ziccardi, L.G.; Fearnside, P.M. Deforestation dynamics in Brazil´s Amazonian settlements: Effects of land-tenure concentration. *J. Environ. Manage.*, **2020**, *268*, 110555. DOI: 10.1016/j.jenvman.2020.110555.

13. INPE. Terrabrasilis. Available on line: http://terrabrasilis.dpi.inpe.br/en/home-page/ (accessed on 30 August 2020).

14. Azevedo-Ramos, C.; Moutinho, P. No man's land in the Brazilian Amazon: Could undesignated public forests slow Amazon deforestation? *Land Use Policy*, **2018**, *73*, 125–127. DOI: 10.1016/j.landusepol.2018.01.005.

15. Souza Jr., C.M.; Shimbo, J.Z.; Rosa, M.R.; Parente, L.L.; Alencar, A.A.; Rudorff, B.F.T.; Hasenack, H.; Matsumoto, M.; Ferreira, L.G.; Souza-Filho, P.W.M. et al. Reconstructing three decades of land use and land cover changes in Brazilian biomes with Landsat archive and Earth Engine. *Remote Sens.*, **2020**, *12*, 2735. DOI: 10.3390/rs12172735.

16. Soares-Filho, B.S.; Nepstad, D.C.; Curran, L.M.; Cerqueira, G.C.; Garcia, R.A.; Ramos, C.A.; Voll, E.; McDonald, A.; Lefebvre, P.; Schlesinger, P. Modelling conservation in the Amazon basin. *Nature*, **2006**, *440*, 520–523. DOI: 10.1038/nature04389.

17. West, T.A.; Börner, J.; Sills, E.O.; Kontoleon, A. Overstated carbon emission reductions from voluntary REDD+ projects in the Brazilian Amazon. *Proc. Natl. Acad. Sci.* **2020**, *117*, 24188–24194. DOI: 10.1073/pnas.2004334117.

18. United Nations Climate Change. Copenhagen Climate Change Conference. Available online: https://unfccc.int/process-and-meetings/conferences/past-conferences/copenhagen-climate-change-conference-december-2009/copenhagen-climate-change-conference-december-2009 (accessed 19 November 2020).

19. Law No. 12.727, 17 October 2012. Available online: http://www.planalto.gov.br/ccivil_03/_ato2011-2014/2012/lei/l12727.htm (accessed on 19 November 2020).

20. Sorrensen, C.L. Linking small holder land use and fire activity: examining biomass burning in the Brazilian Lower Amazon. *For. Ecol. Manag.*, **2000**, *128*, 11–25. DOI: 10.1016/S0378-1127(99)00283-2.

21. Asner, G.P.; Knapp, D.E.; Broadbent, E.N.; Oliveira, P.J.C.; Keller, M.; Silva, J.N. Selective logging in the Brazilian Amazon. *Sci.*, **2005**, *310*, 480–482. DOI: 10.1126/science.1118051.

22. Broadbent, E.N.; Asner, G.P.; Keller, M.; Knapp, D.E.; Oliveira, P.J.C.; Silva, J.N. Forest fragmentation and edge effects from deforestation and selective logging in the Brazilian Amazon. *Biol. Conserv.*, **2008**, *141*, 1745–1757. DOI: 10.1016/j.biocon.2008.04.024.

23. Barber, C.P.; Cochrane, M.A.; Souza Jr., C.M.; Laurance, W.F. Roads, deforestation, and the mitigating effect of protected areas in the Amazon. *Biol. Conserv.*, **2014**, *177*, 203–209. DOI: 10.1016/j.biocon.2014.07.004.

24. Alencar, A.; Nepstad, D.; Diaz, M.C.V. Forest understory fire in the Brazilian Amazon in ENSO and non-ENSO years: area burned and committed carbon emissions. *Earth Interact.*, **2006**, *10*, 1–17. DOI: 10.1175/EI150.1.

25. Matricardi, E.A.T.; Skole, D.; Pedlowski, M.A.; Chomentowski, W.; Fernandes, L.C. Assessment of tropical forest degradation by selective logging and fire using Landsat imagery. *Remote Sens. Environ.*, **2010**, *114*, 1117–1129. DOI: 10.1016/j.rse.2010.01.001.

26. Barni, P.E.; Pereira, V.B.; Manzi, A.O.; Barbosa, E.I. Deforestation and forest fires in Roraima and their relationship with phytoclimatic regions in the northern Brazilian Amazon. *Environ. Manage.*, **2015**, *55*, 1124–1138. DOI: 10.1007/s00267-015-0447-7.

27. Pinheiro, T.F.; Escada, M.I.S.; Valeriano, D.M.; Hostert, P.; Gollnow, F.; Müller, H. Forest degradation associated with logging frontier expansion in the Amazon: The BR-163 region in southwestern Pará, Brazil. *Earth Interact.*, **2016**, *20*, 1–26. DOI: 10.1175/EI-D-15-0016.1.

28. Arima, E.Y.; Walker, R.T.; Perz, S.G.; Caldas, M. Loggers and forest fragmentation: Behavioral models of road building in the Amazon basin. *Ann. Am. Assoc. Geogr.*, **2005**, *95*, 525–541. DOI: 10.1111/j.1467-8306.2005.00473.x.

29. Souza, G.M.; Escada, M.I.S.; Capanema, V.P. Cicatrizes de queimadas e padrões de mudanças de uso e cobertura da terra no sudoeste do estado do Pará, Brasil. In Proceedings of the XVIII Simpósio Brasileiro de Sensoriamento Remoto (SBSR), Santos, Brazil, **2017**, 5760–5767.

30. Butt, N.; Oliveira, P.A.; Costa, M.H. Evidence that deforestation affects the onset of the rainy season in Rondônia, Brazil. *J. Geophys. Res.*, **2011**, *116*, 2–9. DOI: 10.1029/2010JD015174.

31. Knox, R.; Bisht, G.; Wang, J.; Bras, R.L. Precipitation variability over the forest-to-nonforest transition in Southwestern Amazonia. *J. Clim.*, **2011**, *24*, 2368–2377. DOI: 10.1175/2010JCLI3815.1.

32. Davidson, E.A.; Araújo, A.C.; Artaxo, P.; Balch, J.K.; Brown, I.F.; Bustamante, M.M.C.; Coe, M.T.; DeFRIES, R.S.; Keller, M.; Longo, M.; Munger, J.W.; Schroeder, W.; Soares-Filho, B.S.; Souza, C.M.; Wofsy, S.C. The Amazon basin in transition. *Nature*, **2012**, *481*, 321–328. DOI: 10.1038/nature10717.

33. Jiménez-Muñoz, J. C.; Mattar, C.; Barichivich, J.; Santamaría-Artigas, A.; Takahashi, K.; Malhi, Y.; Sobrino A.J.; Van Der Schrier, G. Record-breaking warming and extreme drought in the Amazon rainforest during the course of El Niño 2015–2016. *Sci. Rep.*, **2016**, *6*, 1–7. DOI: 10.1038/srep33130.

34. Zemp, D.C.; Schleussner, C.F.; Barbosa, H.; Rammig, A. Deforestation effects on Amazon forest resilience. *Geophys. Res. Lett.*, **2017**, *44*, 6182–6190. DOI: 10.1002/2017GL072955.

35. Aragão, L.E.; Anderson, L.O.; Fonseca, M.G.; Rosan, T.M.; Vedovato, L.B.; Wagner, F.H.; Silva, C.V.J.; Junior, C.H.S.; Arai, E.; Aguiar, A.P.; Barlow, J.; Berenguer, E.; Deeter, M.N.; Domingues, L.G.; Gatti, L.; Gloor, M.; Malhi, Y.; Marengo, J.A.; Miller, J.B.; Phillips, O.L.; Saatchi, S. 21st Century drought-related fires counteract the decline of Amazon deforestation carbon emissions. *Nat. Commun.*, **2018**, *9*, 1–12. DOI: 10.1038/s41467-017-02771-y.

36. Fearnside, P.M.; Graça, P.M.L.D.A.; Keizer, E.W.H.; Maldonado, F.D.; Barbosa, R.I.; Nogueira, E.M. Modelagem de desmatamento e emissões de gases de efeito estufa na região sob influência da rodovia Manaus-Porto Velho (BR-319). Rev. Bras. Meteorol., **2009**, *24*, 208–233. DOI: 10.1590/S0102-77862009000200009.

37. Aragão, L.E.O.C.; Shimabukuro, Y.E. The incidence of fire in Amazonian forests with implications for REDD. *Science*, **2010**, *328*, 1275–1278. DOI: 10.1126/science.1186925.

38. Hosonuma, N.; Herold, M.; Sy, V.; de Fries, R.S.; Brockhaus, M.; Verchot, L.; Angelsen, A.; Romijn, E. An assessment of deforestation and forest degradation drivers in developing countries. *Environ. Res. Lett.*, **2012**, 7, 044009. DOI: 10.1088/1748-9326/7/4/044009.

39. Spracklen, D.V.; Garcia-Carreras, L. The impact of Amazonian deforestation on Amazon basin rainfall. *Geophys. Res. Lett.*, **2015**, *42*, 9546–9552. DOI: 10.1002/2015GL066063.

40. Jusys, T. Fundamental causes and spatial heterogeneity of deforestation in Legal Amazon. *Appl. Geogr.*, **2016**, *75*, 188–199. DOI: 10.1016/j.apgeog.2016.08.015.

41. Ruiz-Vásquez, M.; Arias, P.A.; Martínez, J.A.; Espinoza, J.C. Effects of Amazon basin deforestation on regional atmospheric circulation and water vapor transport towards tropical South America. *Clim. Dyn.*, **2020**, *54*, 4169–4189. DOI: 10.1007/s00382-020-05223-4.

42. Krieger-Filho, G.C.; Bufacchi, P.; Santos, J.C.; Veras, C.A.G.; Alvarado, E.C.; Mell, W.; Carvalho Jr., J.A. Probability of surface fire spread in Brazilian rainforest fuels from outdoor experimental measurements. *Eur. J. Forest Res.*, **2017**, *136*, 217–232. DOI: 10.1007/s10342-016-1023-2.

43. Carvalho Jr., J.A.; Veras, C.A.G.; Alvarado, E.C.; Sandberg, D.V.; Leite, S.J.; Gielow, R.; Rabelo, E.R.C.; Santos, J.C. Understory fire propagation and tree mortality on adjacent areas to an Amazonian deforestation fire. *Int. J. Wildland Fire*, **2010**, *19*, 795–799. DOI: 10.1071/wf08047.

44. Silva Júnior, C.H.L.; Aragão, L.E.O.; Fonseca, M.G.; Almeida, C.T.; Vedovato L.B.; Anderson, L.O. Deforestation-induced fragmentation increases forest fire occurrence in central Brazilian Amazonia, *Forests*, **2018**, 9, 305, DOI:10.3390/f9060305.

45. Carvalho Jr., J.A.; Higuchi, N.; Araújo, T.M.; Santos, J.C. Combustion completeness in a rainforest clearing experiment in Manaus, Brazil. *J. Geophys. Res.*, **1998**, *103*, 13195–13199. DOI:10.1029/98jd00172.

46. Carvalho Jr., J.A.; Costa, F.S.; Veras, C.A.G.; Sandberg, D.V.; Alvarado, E.C.; Gielow, R.; Serra, A.M.; Santos, J.C. Biomass fire consumption and carbon release rates of rainforest-clearing experiments conducted in northern Mato Grosso, Brazil. *J. Geophys. Res.*, **2001**, *106*, 17877–17887. DOI: 10.1029/2000jd900791.

47. Carvalho, E.R.; Veras, C.A.G.; Carvalho Jr., J.A. Experimental investigation of smouldering in biomass. *Biomass & Bioenerg.*, **2002**, *22*, 283–294. DOI: 10.1016/S0961-9534(02)00005-3.

48. Rabelo, E.R.C.; Veras, C.A.G.; Carvalho Jr., J.A.; Alvarado, E.C.; Sandberg, D.V.; Santos, J.C. Log smoldering after an Amazonian deforestation fire. *Atmos. Environ.*, **2004**, *38*, 203–211. DOI: 10.1016/j.atmosenv.2003.09.065.

49. Carvalho Jr., J.A.; Veras, C.A.G.; Alvarado, E.C.; Gielow, R.; Lincoln, E.N.; Christian, T.J.; Yokelson, R.J.; Santos, J.C. Biomass consumption and CO_2, CO and main hydrocarbon gas emissions in an Amazonian forest clearing fire. *Atmos. Environ.*, **2009**, *43*, 438–446. DOI: 10.1016/j.atmosenv.2008.07.063.

50. Carvalho Jr., Amaral, S.S.; Costa, M.A.M.; Soares Neto, T.G.; Veras, C.A.G.; Costa, F.S.; van Leeuwen, T.T.; Krieger Filho, G.C.; Tourigny, E.; Forti, M.C.; Fostier, A.H.; Siqueira, M.B.; Santos, J.C.; Lima, B.A.; Cascão, P.; Ortega, G.; Frade Jr., E.F. CO_2 and CO emission rates from three forest fire controlled experiments in Western Amazonia. *Atmos. Environ.*, **2016**, *135*, 73–83. DOI: 10.1016/j.atmosenv.2016.03.043.

51. van Marle, M.J.E.; Field, R.D.; van der Werf, G.R.; Wagt, I.A.E.; Houghton, R.A.; Rizzo, L.V.; Artaxo, P.; Tsigaridis, K. Fire and deforestation dynamics in Amazonia (1973-2014). *Global Biogeochem. Cycles*, **2017**, *31*, 24–38. DOI: https://doi.org/10.1002/2016GB005445.

52. Soares Neto, T.G.; Carvalho Jr., J.A.; Veras, C.A.G.; Alvarado, E.C.; Gielow, R.; Lincoln, E.N.; Cristian, T.J.; Yokelson, R.J.; Santos; J.C. Biomass consumption, CO_2, CO and main hydrocarbon gas emissions in an Amazonian forest clearing fire. *Atmos. Environ.*, **2008**, *43*, 438–446. DOI:10.1016/j.atmosenv.2008.07.063.

53. ESA. EO Browser. Available online: https://apps.sentinel-hub.com/eo-browser/ (accessed on 20 November 2020).

54. Assis, L.F.F.G.; Ferreira, K.R.; Vinhas, L.; Maurano, L.; Almeida, C.; Carvalho, A.; Rodrigues, J.; Maciel, A.; Camargo, C. TerraBrasilis: A spatial data analytics infrastructure for large-scale thematic mapping. *ISPRS Int. J. GeoInf.*, **2019**, *8*, 513. DOI: 10.3390/ijgi8110513.

55. INPE. Monitoramento de queimadas e incêndios por satélite em tempo quase-real. Available online: http://queimadas.dgi.inpe.br/queimadas/portal (accessed on 31 August 2020).

56. Giglio, L.; Descloitres, J.; Justice, C.O.; Kaufman, Y.J. An enhanced contextual fire detection algorithm for MODIS. *Remote Sens. Environ.* **2003**, 87, 273–282. DOI: 10.1016/S0034-4257(03)00184-6.

57. Giglio, L.; Schroeder, W.; Justice, C.O. The collection 6 MODIS active fire detection algorithm and fire products. *Remote Sens. Environ.*, **2016**, *178*, 31–41. DOI: 10.1016/j.rse.2016.02.054.

58. Di Biase, V.; Laneve G.; Geostationary sensor based forest fire detection and monitoring: An improved version of the SFIDE algorithm. *Remote Sens.*, **2018**, *10*, 741. DOI: 10.3390/rs10050741.

59. Kaufman, Y.J.; Justice, C.O.; Flynn, L.P.; Kendall, J.D.; Prins, E.M.; Giglio, L.; Ward, D.E.; Menzel, W.P.; Setzer, A.W. Potential global fire monitoring from EOS-MODIS. *J. Geophys. Res. Atmos.* **1998**, *103*, 32215-32238. DOI: 10.1029/98JD01644.

60. Justice, C.O.; Giglio, L.; Korontzi, S.; Owens, J.; Morisette, J.T.; Roy, D.; Descloitres, J.; Alleaume, S.; Petitcolin, F.; Kaufman, Y. The MODIS fire products. *Remote Sens. Environ.* **2002**, *83*, 244–262. DOI: 10.1016/S0034-4257(02)00076-7.

61. Hantson, S.; Padilla, M.; Corti, D.; Chuvieco, E. Strengths and weaknesses of MODIS hotspots to characterize global fire occurrence. *Remote Sens. Environ.*, **2013**, *131*, 152–159. DOI: 10.1016/j.rse.2012.12.004.

62. Silva, C.A.; Santilli, G.; Sano, E.E.; Rodrigues, S.W.P. Análise qualitativa do desmatamento na Floresta Amazônica a partir de sensores SAR, óptico e termal. *Anuário do Instituto de Geociências*, **2019**, *42*, 18–29. DOI: http://dx.doi.org/10.11137/2019_4_18_29.

63. Santana, N.C.; Carvalho Júnior, O.A.; Gomes, R.A.T.; Guimarães, R.F. Burned-area detection in Amazonian environments using standardized time series per pixel in MODIS data. *Remote Sensing*, **2018**, *10*, 1904. DOI:10.3390/rs10121904.

64. Soares-Filho, B.; Rajão, R.; Macedo, M.; Carneiro, A.; Costa, W.; Coe, M.; Rodrigues, H.; Alencar, A. Cracking Brazil's forest code. *Science*, **2014**, *344*, 363–364. DOI: 10.1126/science.1246663.

65. Silva, S.S.; Fearnside, P.M.; Graça, P.M.L.A.; Brown, I.F.; Alencar, A.; Melo, A.W.F. Dynamics of forest fires in the southwestern Amazon. *For. Ecol. Manag.*, **2018**, *424*, 312–322. DOI: 10.1016/j.foreco.2018.04.041.

66. Matricardi, E.A.T.; Skole, D.L.; Costa, O.B.; Pedlowski, M.A.; Samek, J.H.; Miguel, E.P. Long-term forest degradation surpasses deforestation in the Brazilian Amazon. *Science*, **2020**, 369, 6509, 1378–1382. DOI: 10.1126/science.abb3021.

67. Pulselli, R.M.; Romano, P.; Marchi, M.; Bastianoni, S. Carbon emission intensity and areal empower density: Combining two systemic indicators to inform the design and planning of sustainable energy landscapes. Chapter 19. In: *Sustainable Energy Landscapes: Designing, Planning, and Development*, Stremke, S., van den Dobbelsteen, A. (Eds.), CRC Press: Boca Raton, 2013, pp. 385–406.

68. Smith, C.C.; Espírito-Santo, F.D.B.; Healey, J.R.; Young, P.J.; Lennox, G.D.; Ferreira, J.; Barlow, J. Secondary forests offset less than 10% of deforestation-mediated carbon emissions in the Brazilian Amazon, *Glob. Change Biol.*, **2020**, *26*, 7006–7020. DOI: 10.1111/gcb.15352.

69. Laneve, G.; Cadau, E.G.; Santilli, G. Estimation of the burned biomass based on the quasi-continuous MSG/SEVIRI Earth observation system. In *Proceedings of the IEEE International Geoscience and Remote Sensing Symposium (*IGARSS 2009), Cape Town, South Africa, July 12-19, 2009.